The subtropical ridge in CMIP5 models, and implications for projections of rainfall in southeast Australia

Michael Grose[1], Bertrand Timbal[2], Louise Wilson[1], Janice Bathols[1] and David Kent[2]

[1] CSIRO Ocean and Atmosphere Flagship, Aspendale, VIC, Australia
[2] Bureau of Meteorology, Docklands, VIC, Australia

(Manuscript received September 2014; accepted March 2015)

The subtropical ridge (STR) is the mean pressure ridge in the mid-latitudes, and is one of the key features affecting climate variability and change in southeast Australia. Changes to the STR and associated changes to rainfall in a warming climate are of strong interest, and the new Coupled Model Inter-comparison Project phase 5 (CMIP5) model archive provides new opportunities to examine this. Here we show that the STR is projected to strengthen and move pole-ward under global warming, contributing to reduced rainfall in the cool season in southeast Australia. This result is largely consistent among 35 models examined, and CMIP5 shows a greater increase in intensity relative to position than CMIP3 did. We show that the simulation of the STR in the CMIP5 is similar to that of the previous CMIP3 in many respects, including the underestimation of both the historical trends in the STR intensity and the correlation between inter-annual STR intensity and southeast Australian rainfall. These issues mean we still have reduced confidence in regional rainfall projections for southeast Australia and suggest that CMIP5 rainfall projections for this region in April to October may be underestimates.

Introduction

The subtropical ridge (STR) in the southern hemisphere is the region of high mean sea level pressure (MSLP) in the mid latitudes associated with the descending branch of the Hadley circulation. It divides the region of predominantly westerly winds and winter rainfall to its south, and tropical conditions to its north (Peixoto and Oort 1992). Over Australia, the STR is well quantified in the east (~150 °E) due to a relatively high density of MSLP observations. Indices that describe the ridge intensity (STR-I) and position (STR-P) in this region can be used to explore the influence of the STR on southeast Australian rainfall. These indices show an annual cycle with a maximum intensity and northerly extent in June to August and a minimum in intensity in January to February (Figure 1a).

Rainfall variability and trends in southeastern Australia are mainly determined by the incidence of frontal and cutoff weather systems and stream flow, which in turn are linked to large scale circulation (Risbey et al. 2013a). Changes to mid-latitude storm tracks and atmospheric blocking events influence the incidence of rain bearing systems over southern Australia (e.g. Frederiksen and Frederiksen 2011). The STR provides a measure of the high pressure systems that typically lie to the north of the storm tracks and therefore have a role in steering the storm track and the fronts embedded in the westerly flow. The intensity, position and other characteristics of the STR are linked to the frequency and strength of storms and fronts that cross southern Australia , and the STR is therefore an important feature of Australian rainfall variability and change (Pittock 1971; Pittock 1973; Drosdowsky 2005; Larsen and Nicholls 2009; Williams and Stone 2009; Timbal et al. 2010; Timbal and Drosdowsky 2013; Whan et al. 2013). Both the STR-I and STR-P are negatively correlated with rainfall anomalies in southern Australia on an inter-annual timeframe (Figures 1b and 1c). That is, a stronger or more pole-ward STR implies generally lower rainfall, and vice versa. The edge of the tropics affects southern Australian rainfall directly and indirectly via the STR and blocking, and an expansion of the tropics is expected to lead to reduced rainfall in subtropical Australia (Maher and Sherwood 2014). Also, the position and intensity of the STR can reflect remote drivers of rainfall variability in southeast Australia. The Hadley cell tends to shrink and the STR move equator-ward during El Niño events or when the Southern Annular Mode (SAM) is less intense and the opposite tends to occur during La Niña events and when the SAM is intense

Corresponding author address: Michael Grose, CSIRO Ocean and Atmosphere Flagship, Aspendale, Vic, Australia
Email: Michael.Grose@csiro.au

(Nguyen et al. 2013). Also, a positive Indian Ocean Dipole tends to increase the intensity of the STR and push it pole-ward in winter (Cai et al. 2011).

Figure 1 Subtropical ridge (STR) indices and Australian rainfall, (a) Mean annual cycle of the STR-I and STR-P index in 1948-2002 in: BOM observations (blue), NNR (dashed blue), the multi-model mean of CMIP5 models (red), as well as the multi-model mean of CMIP3 models in the 1948-1974 period used by Kent et al. (2013) (note period is different than for CMIP5), (green), months are marked by initial letter; (b) the correlation between the inter-annual variability of annual STR-P in BOM and annual rainfall in AWAP in 1900-2007; (c) as for b but for STR-I. Box shows the region of rainfall calculations (land only is used).

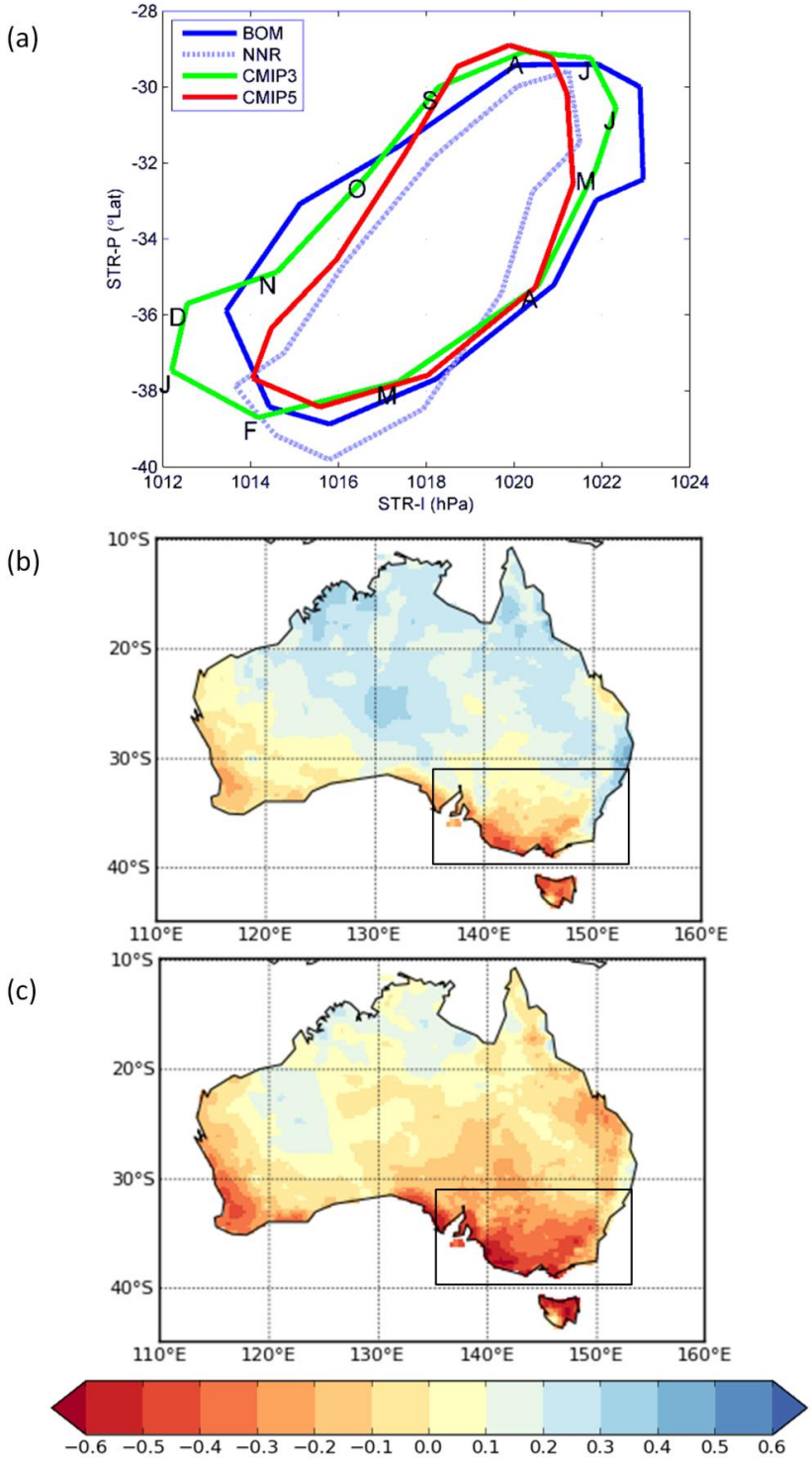

There are various lines of evidence that the STR has intensified and trended poleward during the instrumental record. However, considerable inter-annual and decadal variability make trends difficult to discern. Studies have detected a poleward shift in the annual STR-P during periods within the record since 1890 (Kidson 1925; Deacon 1953; Das 1956; Pittock 1971; Pittock 1973), including some showing a significant trend (Das 1956; Thresher 2003). However, Drosdowsky (2005) has critiqued some of the methods used in these studies and found no discernible trend. In terms of intensity, there is more clear-cut evidence that the mean STR-I has intensified in recent decades (Timbal and Drosdowsky 2013). A decline in southeast Australian rainfall since the 1970s and a severe drought between 1997 and 2009 (the Millennium Drought) were associated with an intensification of the STR (Larsen and Nicholls 2009; Timbal and Drosdowsky 2013; Whan et al. 2013), but numerous processes may have played a role in the Millennium Drought and the relative role of each one is not completely clear (for example, see Risbey et al. 2013a; Risbey et al. 2013b and references therein). In general, the relationship between inter-annual variability in STR-P and rainfall is weaker than that for the STR-I (Larsen and Nicholls 2009; Timbal and Drosdowsky 2013) but there is some interaction between both indices in autumn (Whan et al. 2013).

A consistent finding of theory and model studies is that warming of the climate has led to expansion of the Hadley circulation and a pole-ward movement of the eddy-driven jet of westerlies (Collins et al. 2013b; Lucas et al. 2014 and references therein), and may be a cause of recent changes in the STR (Nguyen et al. 2013). Other forcings such as stratospheric ozone depletion also impart an influence on the STR (Karoly 2003). Kent et al. (2013) found that 23 Global Climate Models (GCMs) in the Coupled Model Inter-comparison Project phase 3 (CMIP3) archive (Meehl et al. 2007)) projected an increase in STR intensity over the 21st Century (median of 0.21 hPa per degree of global warming (PDGW)). All but one model projected a pole-ward movement (median of 0.25° latitude PDGW).

GCMs suffer from both biases in the pressure patterns and the STR-rainfall relationships, creating an impediment to reliable climate projections. By examining where each model simulates a pressure pattern that most closely matches the observations, Kent et al. (2013) noted that five of the 23 CMIP3 models located the STR too far west or defined it as too broad. Other biases were also noted in the mean latitude, mean intensity, annual cycle or inter-annual variability of both the STR-P and STR-I. These biases affect the confidence in projections of MSLP and rainfall because changes of the STR relate to different present-day patterns. Therefore, while many CMIP3 models project a decrease in southern hemisphere rainfall (Christensen et al. 2007) broadly consistent with an intensification and poleward movement in the STR, projections of the magnitude and extent of these decreases is compromised by the model biases. Also, changes in the STR and the expansion of the sub-tropical dry zone has been slower in models than in observations in recent decades (CSIRO 2012).

Furthermore, another difficulty is that some models actually fail to reproduce the observed correlations between the inter-annual variability of the index of STR intensity rainfall in southeast Australia (Kent et al. 2013). This is pertinent to regional rainfall projections for southern Australia, as it suggests that for a given change to the STR, these models will not produce the correct corresponding rainfall change. However, there are some complicating factors to consider. The relationships between indices of the STR and rainfall vary over time (Drosdowsky 2005; Larsen and Nicholls 2009; Whan et al. 2013). The relationship between rainfall and STR intensity is more stable through time than that to STR position, particularly in the peak of the cool season. Because the relationship of STR-P to rainfall "seesaws" between negative and positive between the warm and cool seasons in many parts of southern Australia, there is interplay between the relationship of the two indices to rainfall. In recent decades the mean position of the STR has moved slightly pole-ward, driving the line between positive and negative correlations of rainfall to the STR indices further south (Timbal et al. 2010). That southward shift combined with the annual cycle of relationship leads to some non-linear interactions between the intensity and position of the STR, in particular in the transition season of autumn (Whan et al. 2013). This suggests that in order for climate models to properly capture the complex STR-rainfall relationship in space and time, small biases can pose a problem.

A new set of global climate model experiments (CMIP5) have recently been made available (Taylor et al. 2012) , containing simulations from many more GCMs than CMIP3, and many models that have undergone development. These models project a general reduction in southern Australian rainfall through the century, similar to CMIP3 (Collins et al. 2013a; Collins et al. 2013b). In this study we revisit the issue of the STR in model simulations, including the relationship between the projected changes to rainfall and the STR. Specifically, we are interested in possibly constraining the rainfall projections based on an evaluation how well the STR and rainfall-STR relationships are simulated.

Methods and data

There have been several methods used to calculate the latitude of the STR, including some variants on the *L* index of Pittock (1973). See Drosdowsky (2005) for a review of many of these methods. Several studies have also quantified the STR intensity (Drosdowsky 2005; Larsen and Nicholls 2009; Timbal and Drosdowsky 2013). All methods to quantify the location and intensity of the STR use mean sea level pressure (MSLP), since there are generally long records of fairly high-quality data for this variable. All methods fundamentally calculate a profile of zonal mean MSLP over a particular longitude band and time period, then detect the latitude and magnitude of the MSLP maximum in that profile. The main differences between methods concern the longitude band considered, the curve-fitting method used to detect the maximum pressure, the input dataset used (station data or Reanalysis) and the time interval (daily or monthly). Many methods consider a narrow band centred on 150 °E (e.g. Drosdowsky 2005), but one study considered the breadth of Australia at 110-155 °E (Larsen and Nicholls 2009). Here we follow

the method of Drosdowsky (2005), as adapted for use in climate models by Timbal et al. (2010) and Kent et al. (2013). We interpolate the zonal mean MSLP to 0.5° resolution, fit a cubic spline curve to the data and detect the location and pressure of the maximum in the curve. We focus on the longitude band of 140-150 °E and a latitude range of 9-45 °S. Where the maximum was at the extreme end of the latitude profile, a local search around the maximum of the previous time step was performed.

We examined the mean annual cycle of STR indices calculated from both monthly gridded NCEP/NCAR Reanalysis 1 (NNR), (Kalnay et al. 1996) and the time series based on the updated Bureau of Meteorology monthly station-based time series, referred to as BOM (Timbal and Drosdowsky 2013). No detrending was performed for either dataset, but trends are smaller than both the annual cycle and inter-annual variability so trends do not greatly affect the analysis of these features. The annual cycle of the STR-I and STR-P indices is slightly different in each of these datasets (Figure 1a). BOM uses an interpolation of station observations and NNR uses an atmospheric model fed by the same station observations. The difference between the two reflects the uncertainty of a model to reproduce an index computed from point observations based on daily data. Even if the model product is considered near perfect, it computes a state of the atmosphere based on the model equations but informed by observations. Therefore, the difference between the two datasets represents a tolerance against which models can be evaluated. However, these differences are generally smaller than the differences between observations and models in CMIP3 (Kent et al. 2013). Also, we used only monthly data for all calculations, mindful of the differences to indices calculated from daily data (see Drosdowsky 2005).

Figure 2 The longitude band over Australia where the annual cycle of mean sea level pressure in 1948-2002 most closely matches that in NNR for 140-150 °E for each model, measured by Euclidean distance of the annual cycle

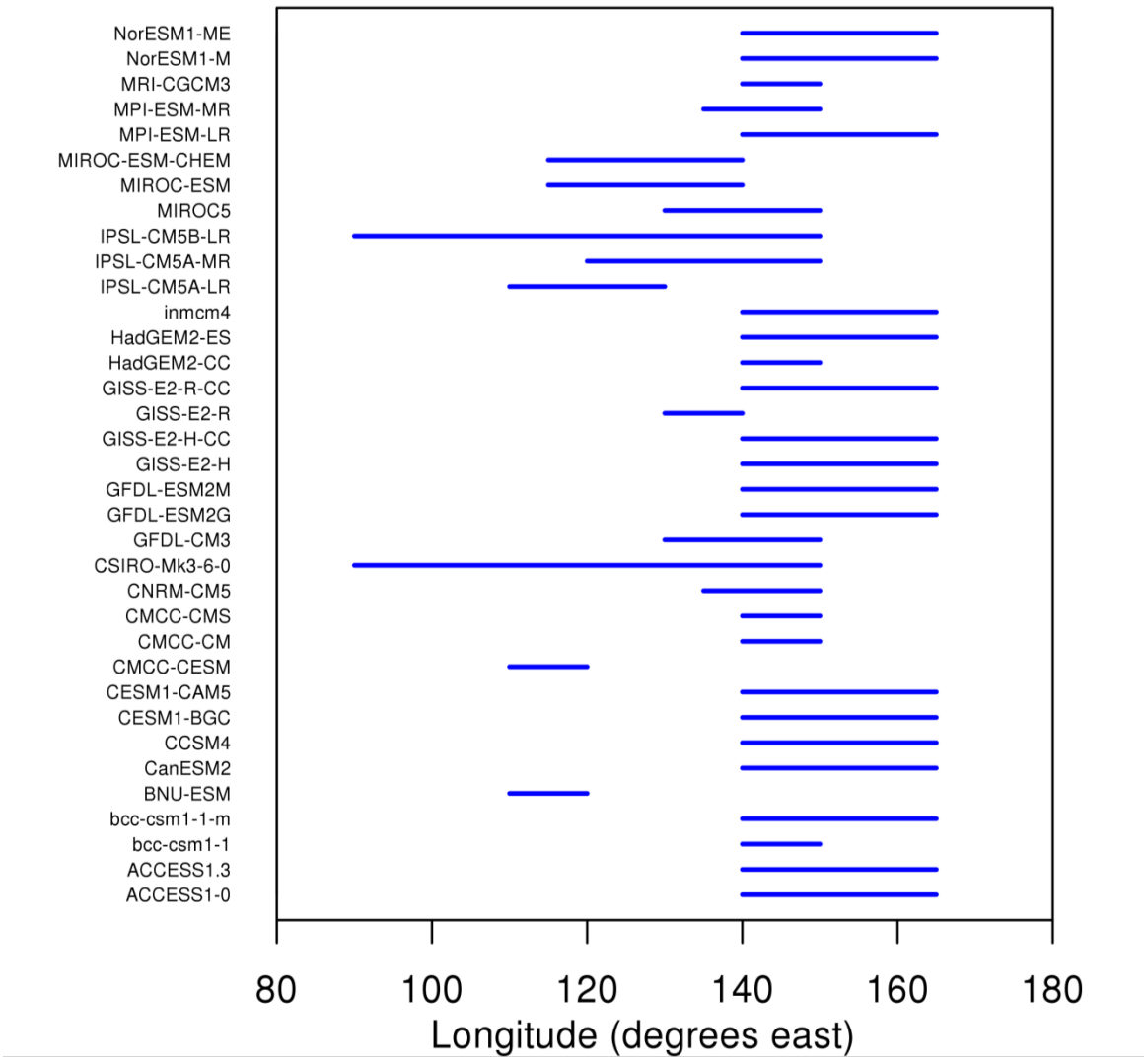

Table 1 The 35 CMIP5 global climate models (GCMs) used in this study. Shown are statistics for the April-October season for the Sub-tropical Ridge Intensity index (STR-I), position index (STR-P) and rainfall in the southeast Australia box (Rainfall, see Figure 1 for box) in models and also observations of BOM STR indices and AWAP rainfall (BOM/AWAP), and NCEP/NCAR Reanalysis 1 (NNR) where appropriate. For each metric, columns show the mean, inter-annual variability (standard deviation, SD) and linear trends for 1948-2002 and 2006-2099. Trends are units per decade (e.g. hPa/decade) and significant trends ($p<0.05$) are shown bold.

	Model	***STR-I (hPa)***				***STR-P (°Lat)***				***Rainfall (mm/month)***			
		Mean	SD	Trend 1948-2002	Trend 2006-2099	Mean	SD	Trend 1948-2002	Trend 2006-2099	Mean	SD	Trend 1948-2002	Trend 2006-2099
	Obs (BOM/AWAP)	1021.1	1.2	**0.22**		-31.57	1.79	-0.08		56.19	12.82	-1.42	
	NNR	1019.6	1.3	**0.26**		-32.24	1.31	-0.01					
	Median of Models	1019.8	0.9	0.02	0.14	-31.34	1.12	-0.05	-0.10	44.59	9.03	-0.20	-0.61
	Model 10th percentile	1018.5	0.7	-0.04	0.06	-32.24	0.60	-0.17	-0.18	35.09	7.67	-1.25	-1.69
	Model 90th percentile	1021.6	1.1	0.14	0.29	-29.17	1.50	0.13	-0.02	63.90	11.61	1.19	0.28
1	ACCESS1.0	1020.0	0.9	0.06	**0.22**	-31.97	1.35	-0.14	0.00	44.29	7.70	-0.82	-0.90
2	ACCESS1.3	1021.3	0.9	-0.06	**0.16**	-31.91	1.07	0.11	**-0.11**	43.06	7.88	-0.52	-2.28
3	BCC-CSM1.1	1020.9	0.7	0.00	**0.14**	-31.25	0.85	0.04	-0.05	46.46	9.03	-0.20	-0.59
4	BCC-CSM1.1(m)	1021.0	0.9	0.09	**0.13**	-31.51	0.78	**-0.14**	**-0.09**	52.45	10.00	0.52	-0.19
5	BNU-ESM	1021.8	0.7	0.04	**0.16**	-30.90	0.69	-0.03	**-0.10**	39.02	10.07	-0.74	-1.71
6	CanESM2	1021.5	1.0	0.09	0.04	-31.34	1.14	-0.09	-0.04	41.90	8.87	0.82	0.15
7	CCSM4	1021.8	1.1	0.07	0.07	-31.64	1.11	-0.11	-0.06	54.29	11.48	1.35	0.54
8	CESM1(BGC)	1021.6	0.9	-0.02	**0.14**	-31.68	1.01	0.03	-0.06	52.52	10.92	0.69	-0.70
9	CESM1(CAM5)	1019.8	0.9	0.10	**0.16**	-31.91	1.11	-0.08	-0.08	46.23	12.83	1.61	-0.27
10	CMCC-CESM	1018.6	0.8	0.03	**0.16**	-29.80	0.57	0.01	**-0.10**	37.45	11.26	-0.36	-1.27
11	CMCC-CM	1019.5	1.0	**0.18**	**0.12**	-30.84	1.20	-0.17	**-0.13**	44.59	8.60	-1.69	-0.02
12	CMCC-CMS	1019.0	1.2	0.17	**0.20**	-29.91	1.49	**-0.27**	**-0.12**	42.73	8.23	0.68	-1.23
13	CNRM-CM5	1020.0	0.9	-0.04	**0.14**	-32.17	1.08	-0.04	-0.10	56.89	13.53	0.33	-1.46
14	CSIRO-Mk3.6.0	1020.4	0.7	0.02	**0.04**	-30.44	0.57	-0.05	**-0.09**	32.00	7.28	0.69	-1.05
15	GFDL-CM3	1019.6	0.8	-0.01	**0.28**	-31.21	0.60	-0.05	**-0.24**	44.40	11.70	0.51	-1.51
16	GFDL-ESM2G	1021.5	0.8	0.02	**0.18**	-31.97	1.34	-0.05	0.03	40.75	8.82	-0.71	-0.79
17	GFDL-ESM2M	1022.8	0.8	0.02	**0.16**	-32.77	1.60	**0.30**	**-0.08**	41.01	12.39	0.37	-1.84
18	GISS-E2-H	1018.1	0.9	0.02	**0.15**	-32.29	1.84	0.10	-0.01	62.31	9.90	-1.08	-0.51
19	GISS-E2-H-CC	1018.5	0.7	-0.03	**0.12**	-31.43	1.50	0.16	**-0.14**	64.94	11.00	-1.23	-0.61
20	GISS-E2-R	1018.1	0.8	-0.03	**0.09**	-31.65	1.34	-0.11	-0.03	61.89	7.65	-0.40	0.14
21	GISS−E2−R−CC	1018.1	0.7	0.03	**0.08**	-31.21	1.13	0.12	-0.02	62.33	9.79	0.33	0.08
22	HadGEM2-CC	1019.8	0.8	0.02	**0.25**	-30.90	1.12	-0.17	-0.10	34.41	7.38	0.34	-0.49
23	HadGEM2-ES	1020.0	1.1	-0.04	**0.31**	-30.90	1.50	0.13	**-0.17**	34.84	7.47	-0.11	-1.34
24	INM-CM4	1021.5	0.7	**-0.12**	**0.06**	-32.62	0.96	**0.16**	-0.06	46.71	9.46	0.18	-0.64
25	IPSL-CM5A-LR	1018.9	1.0	0.14	**0.13**	-29.05	0.83	**-0.20**	**-0.28**	35.47	7.80	-1.75	-1.43
26	IPSL-CM5A-MR	1018.8	1.2	0.09	**0.24**	-28.82	1.01	-0.11	**-0.39**	33.54	7.96	-0.41	-1.66
27	IPSL-CM5B-LR	1018.7	0.9	0.04	**0.03**	-28.69	0.71	-0.09	**-0.13**	42.44	7.69	-1.00	-0.05
28	MIROC5	1019.1	1.1	-0.04	**0.29**	-31.82	1.45	-0.08	-0.06	70.35	10.70	1.63	0.79
29	MIROC−ESM	1019.4	0.7	0.00	**0.32**	-29.11	0.49	-0.04	**-0.18**	73.23	8.39	-1.70	-0.59
30	MIROC−ESM−CHEM	1019.5	0.9	0.14	**0.32**	-29.27	0.61	-0.09	**-0.15**	72.62	8.21	-1.24	-0.49
31	MPI-ESM-LR	1019.6	1.0	0.05	**0.14**	-29.74	1.42	0.10	**-0.12**	40.39	9.97	1.24	-1.06
32	MPI−ESM−MR	1019.2	0.9	0.00	**0.14**	-30.00	1.15	-0.05	-0.07	46.66	9.92	-0.24	-1.94
33	MRI-CGCM3	1021.3	1.0	0.12	**0.06**	-31.70	1.65	-0.22	**-0.12**	41.94	8.29	-0.53	-0.32
34	NorESM1-M	1020.2	1.0	0.13	**0.16**	-32.03	1.38	-0.16	-0.06	48.31	9.66	1.11	0.36
35	NorESM1-ME	1020.5	0.9	-0.05	**0.14**	-32.39	1.35	0.01	**-0.11**	51.82	9.03	-1.26	0.72

Observed rainfall is represented by the Australian Water Availability Project (AWAP) climate dataset (Jones et al. 2009). We refer to rainfall both in gridded form and averaged over a box in southeast Australia (shown in Figure 1b, using land area only), as used in Timbal (2009). Model data is derived from the results of 35 CMIP5 models (Table 1). We used Run 1 from the historical simulations and the representative concentration pathway RCP8.5 (van Vuuren et al. 2011) experiments. We examined the STR indices at longitude bands of all widths and locations at 10 °E increments between 90-180 °E and detected where the models simulated an annual cycle of pressure that matched that in NNR at 140-150 °E (after Kent et al. 2013). The band that most closely matched observations was used to examine STR indices.

For examining past and projected rainfall changes, we focussed on the 7-month cool season April-October when the influence of the STR is strongest (Timbal and Drosdowsky 2013). Linear trends in STR indices and rainfall were examined over two periods; 1948-2002 and 2006-2099 and the relationship of STR indices and rainfall are shown for 1950-1999 and 2050-2099.

Results

Evaluation

The correlation between the inter-annual variability in AWAP annual rainfall and both the annual STR-I (Figure 1b) and STR-P (Figure 1c) index from BOM in 1900-2007 is most strongly negative over southeast Australia and the Australian Alps and positive in some regions north of 30 °N. Negative correlations are generally stronger and more widespread for intensity rather than position. This correlation varies only slightly for different datasets and the period it is calculated over. Despite the noticeable difference in the annual cycle of the STR in the BOM dataset and NNR (Figure 1a), there are only small differences between the maps of correlation to rainfall anomalies using the two dataset (not shown). Notably, correlations are less widespread and weaker when a short recent period is considered (1986-2005). This last point is important to note when considering model results, as climate models generated their own internal variability which is not timed to the observed one.

The annual cycle of MSLP in 10°-wide bands between 90 and 180 °E that matches that in NNR at 140-150 °E in 1948-2002 was identified for each model (Figure 2). We then identified the range of longitudes over which the Euclidean difference with the observed annual cycle was a minimum (Figure 2) (as per Kent et al. 2013). Many models reproduce the cycle in a region roughly around 140-150 °E, but others produce it over different bands. Kent et al. (2013) suggested that models with a band that is 40° or wider (the 'width' criterion) or where the location does not reach 140 °E (the 'location' criterion) are candidates for rejection. Based on these criteria, we identified 6 such models: three based on the width criterion (CMCC-CESM, CSIRO-Mk3.6 and IPSL-CM5B-LR) and three based on the location criterion (BNU-ESM, IPSL-CM5A-LR and MIROC-ESM). The width and location of this band is very similar in 1986-2005 in most models (not shown), suggesting that the general model behaviour is more consistent through time than natural variability.

The multi-model mean of all 35 models examined here shows an annual cycle fairly consistent with observations, lying between BOM and NNR in most months of the year but with a slight northerly bias in August and September (Figure 1a). The bias in the CMIP5 mean is less than in the CMIP3 mean in some respects, but is not reduced all year round. A notable difference is the absence of the low intensity bias in December and January in CMIP5 that was present in CMIP3. This difference is not due to the different time periods considered, as CMIP3 still shows a low bias in summer later in these months in the 21st Century. There is a range of different biases present in the various models (see Additional Material A for each model).

Mean values of the indices during the cool season (April-October) are shown in Table 1. The BOM and NNR each give a slightly different estimate of STR-P, but many CMIP5 models place the STR further north than both (Table 1), as was the case in CMIP3. The simulated intensity in April-October is generally too weak compared to the BOM and NNR values (Table 1). Table 1 also compares observed and simulated April-October rainfall for the southeast Australian region. Both the absolute values and the inter-annual variability are too low in most models compared to the observations (AWAP) although some models are higher.

The spatial pattern of the correlation between April to October rainfall and the STR-I in April to October (AMJJASO) varies considerably between models, with some considerable differences to the observed pattern (Figure 1c). Figure 3 compares the patterns from the 5 models that best match the observed STR (BCC-CSM-1, CMCC-CM, CMCC-CMS, HadGEM2-CC, MRI-CGCM3), the 6 models that perform worst (BNU-ESM, CMCC-CESM, CSIRO-Mk3.6, IPSL-CM5A-LR, IPSL-CM5B-LR, MIROC-ESM). While the coarse horizontal resolution of some models impedes an exact match, some of the higher resolution models reproduce some realistic regional detail (e.g. MRI-CGCM3). There is not a clear difference between the six poor models and other models in terms of correlation to rainfall. A sampling of other models shows some more diversity across CMIP5 (Figure 3, middle column), including some that show a positive correlation over some regions of southern Australia (e.g. ACCESS-1.3, CanESM2, MPI-ESM-LR). Numerous CMIP3 models also showed regions of positive correlation in southeast Australia. For all models see Additional Material B.

Focussing on the monthly rainfall over the southeast Australian box, we see that the correlations with the STR-I is generally too weak in models throughout the cool season, especially between April and August (Figure 4a). Similarly, the correlation of rainfall with the STR-P is much

weaker than observed in many models, especially between July and November (Figure 4b). However, the correlation between the two indices is similar to observed (Figure 4c).

Figure 3 Correlation of STR-I to annual rainfall anomaly in 1948-2002 in BOM STR-I and AWAP rainfall, as well as 21 example models from CMIP5 including (left) models that matched NNR in Figure 2, (middle) assorted models and (right) models that failed the STR evaluation tests.

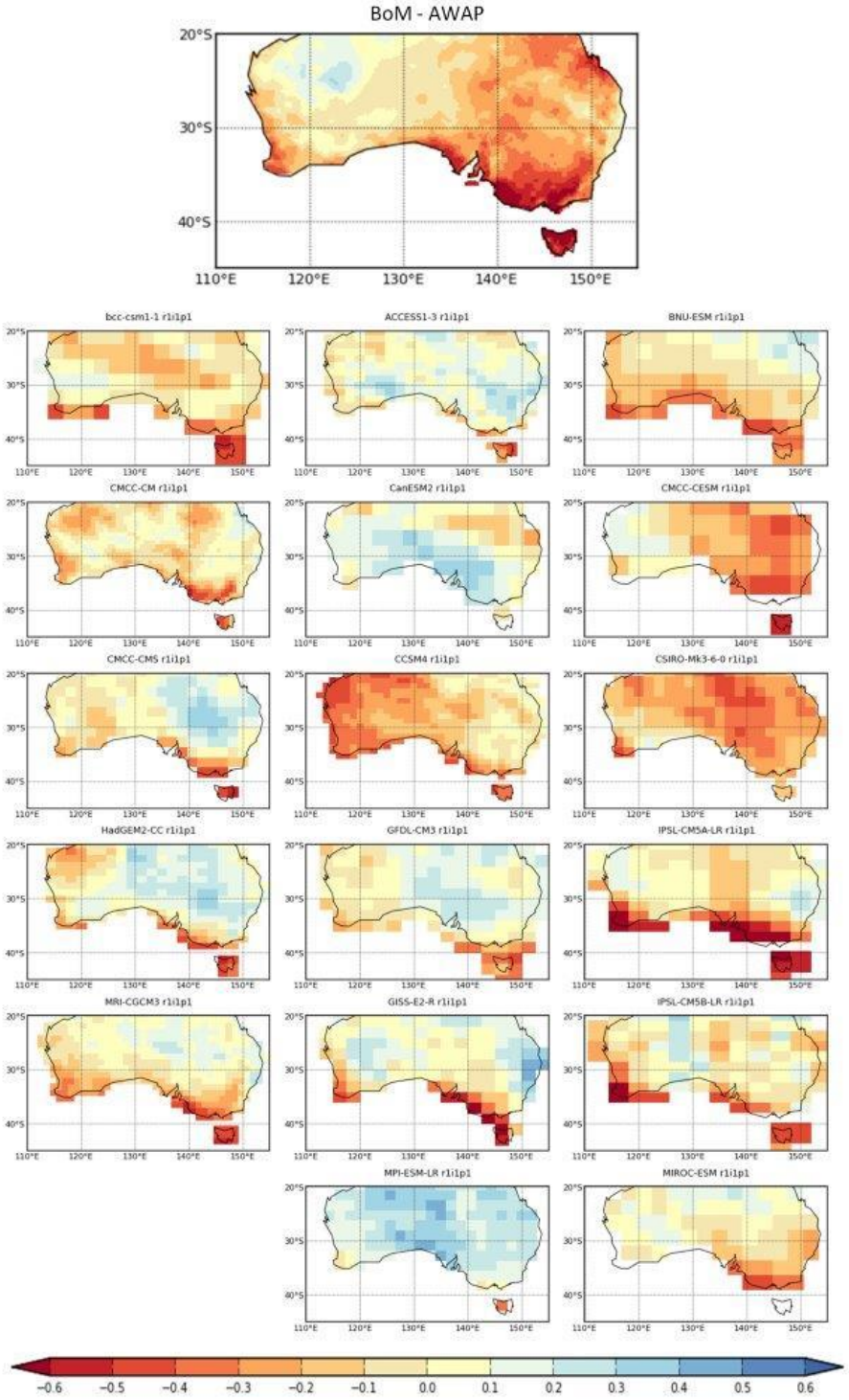

Figure 4 Correlation between STR-P, STR-I and rainfall for SE Australia (box marked in Figure 1) for 1948-2002 from 35 CMIP5 models (grey), the model mean (red), and BOM indices and AWAP rainfall (black)

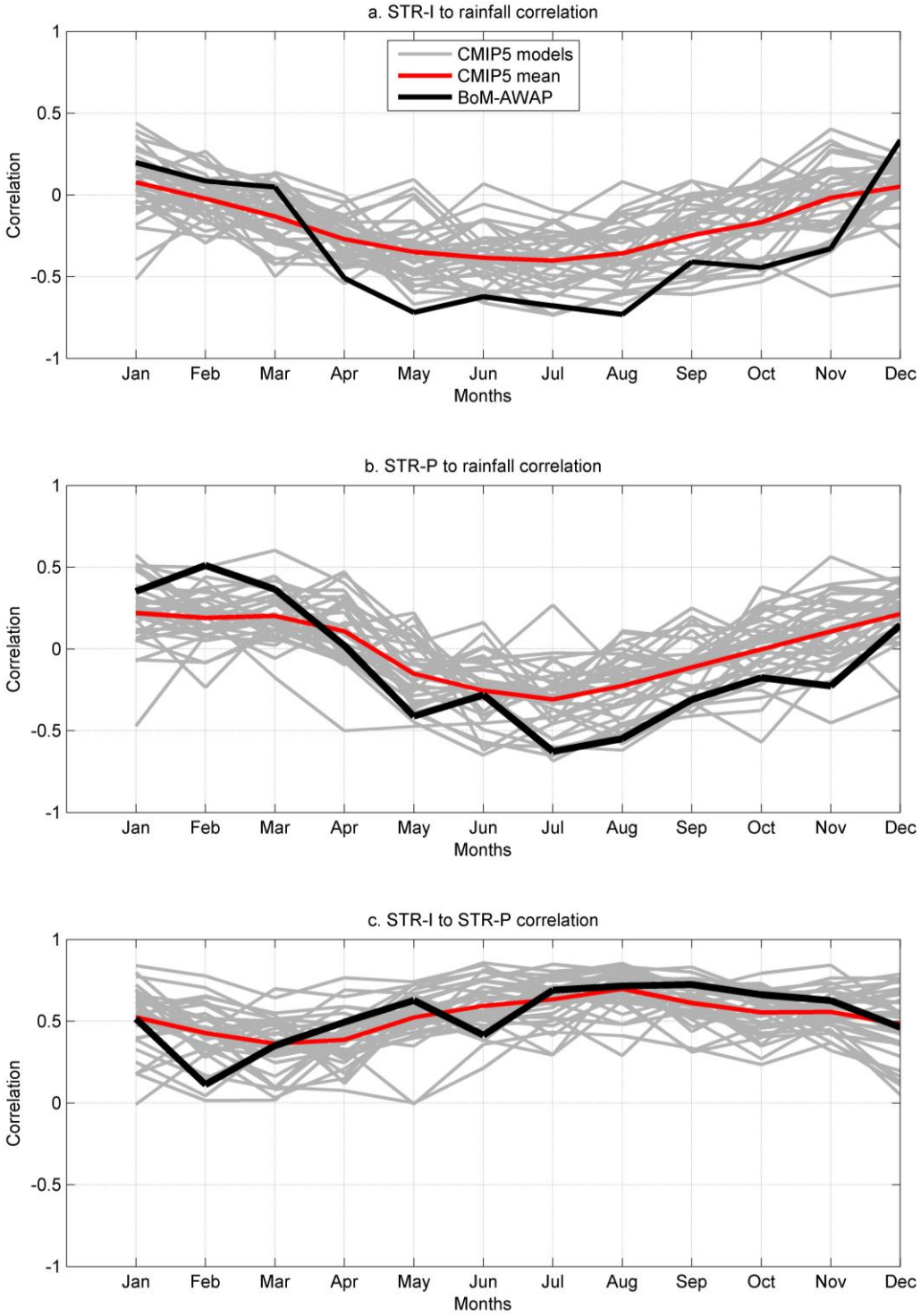

The trend (1948 to 2002) in April-October STR-I between 1948 and 2002 is similar in both observed data sets (+0.22 hPa/decade in BOM and +0.26 hPa/decade in NNR) despite the mean intensities being different (Table 1). Trends are significant in both. Most CMIP5 models simulate a intensification but in all cases the trend is smaller than observed (model median +0.02 hPa/decade, Table 1), and not significant in most cases. The trend is actually negative in 10 of the 35 models. The CMIP3 models also underestimated the observed STR-I strengthening in recent decades. If we scale the trends in STR-I by the associated average global temperature change we find that for the global warming of +0.55 °C in

1948-2002 the observed trend is +2.16 hPa PDGW (BOM) and +2.6 hPa PDGW (NNR). For the global warming of 0.84 °C in 1890-2013, the trend is +2.26 hPa PDGW (BOM). The CMIP5 trends are again much lower, with a median value of only+0.44 hPa PGDW (Table 1).

There is a slight poleward shift in the STR between 1948 and 2002 in BOM data (trend -0.08 °Lat/decade) which is not as evident in NNR (trend of -0.01 °Lat/decade), however we find neither trend is significant to the 95% level over this period (Table 1). The BOM and NNR datasets use different data inputs and modelling techniques, so give different results. Also, recent trends in the Hadley Cell intensity and width differ in different reanalyses datasets due to factors such as different model physics schemes and data assimilation procedures (Nguyen et al. 2013). It is not possible to isolate which is the most accurate estimate among these different datasets. There is a range of trends in STR-P in the CMIP5 results (median of models -0.05 °Lat/decade), with significant trends in only a few cases and 12 models indicating an equator-ward shift (Table 1). Scaled by warming, the model median trend (-0.1 °Lat PDGW) is markedly lower than the BOM-based rate of -0.78 °Lat PDGW but similar to the NNR-based rate of -0.11 °Lat PDGW.

The trend in southeast Australian April-October rainfall in AWAP in 1948-2002 (-1.42 mm/month/decade, Table 1) is underestimated in all CMIP5 models (model median of -0.2 mm/month/decade), with some models exhibiting a positive trend (Table 1).

Projected changes

The multi-model mean of CMIP5 model results under RCP8.5 indicates a progressive strengthening and southern shift of the STR by the end of the century (Figure 5). In most models there is a stronger and more significant projected increase in STR-I (model median +0.14 hPa/decade) than in recent decades, and a clearer projected trend in STR-P (model median -0.10 °Lat/decade) than in recent decades (although many do not show significant trends). All trends in STR-I are positive and trends in STR-P are pole-ward in all but one model, however changes in some models are small (Table 1). Scaled by the projected warming in each model, the model median trend over 2006 to 2099 is +0.37 hPa PDGW, which is similar to that simulated over the recent past (+0.43 hPa PDGW), except with fewer outliers caused by low signal to noise (Figure 6). The median trend in STR-P is -0.21 °Lat PDGW, which is stronger than that simulated over the recent past (-0.11 °Lat PDGW). The equivalent projections from 23 CMIP3 models were +0.21 hPa and -0.25° latitude per PDGW (Kent et al. 2013). The newer models therefore tend to project a greater intensification of the STR and a slightly smaller poleward shift compared to CMIP3.

Figure 5 Model projection of annual cycle of STR-I and STR-P in historical simulations for 1948-2002, and for the middle and end of the 21st Century under RCP8.5 (months marked by initial letter).

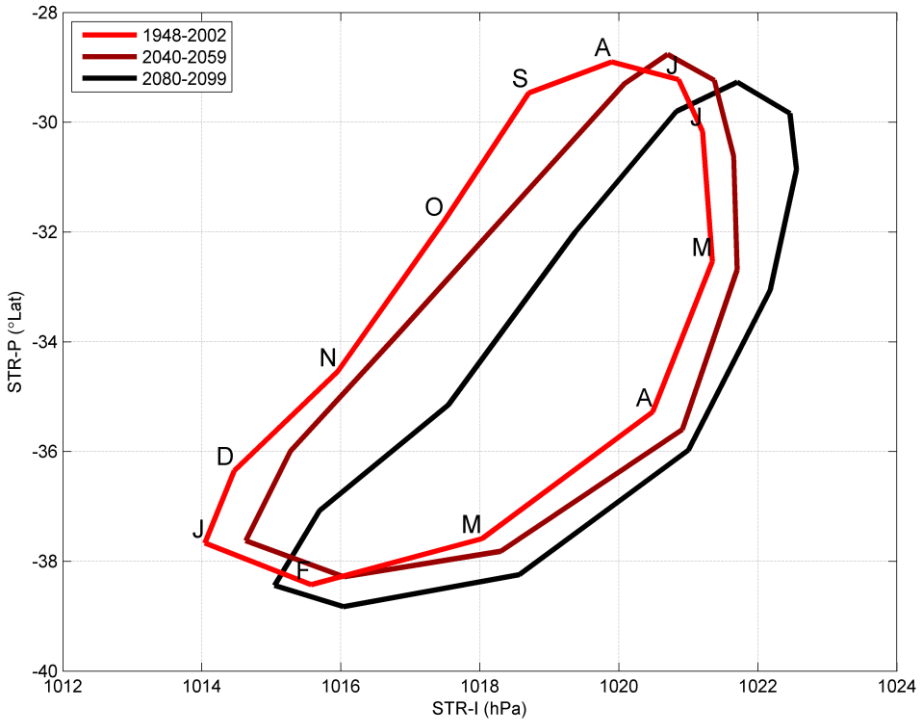

Figure 6 Trends per degree global warming (PDGW) in (a) STR-P and (b) STR-I, in BOM, NNR and 35 CMIP5 models in the past period (1948-2002) and model projections for RCP8.5 (2006-2099). Models are shown in order of the projected trend in each index.

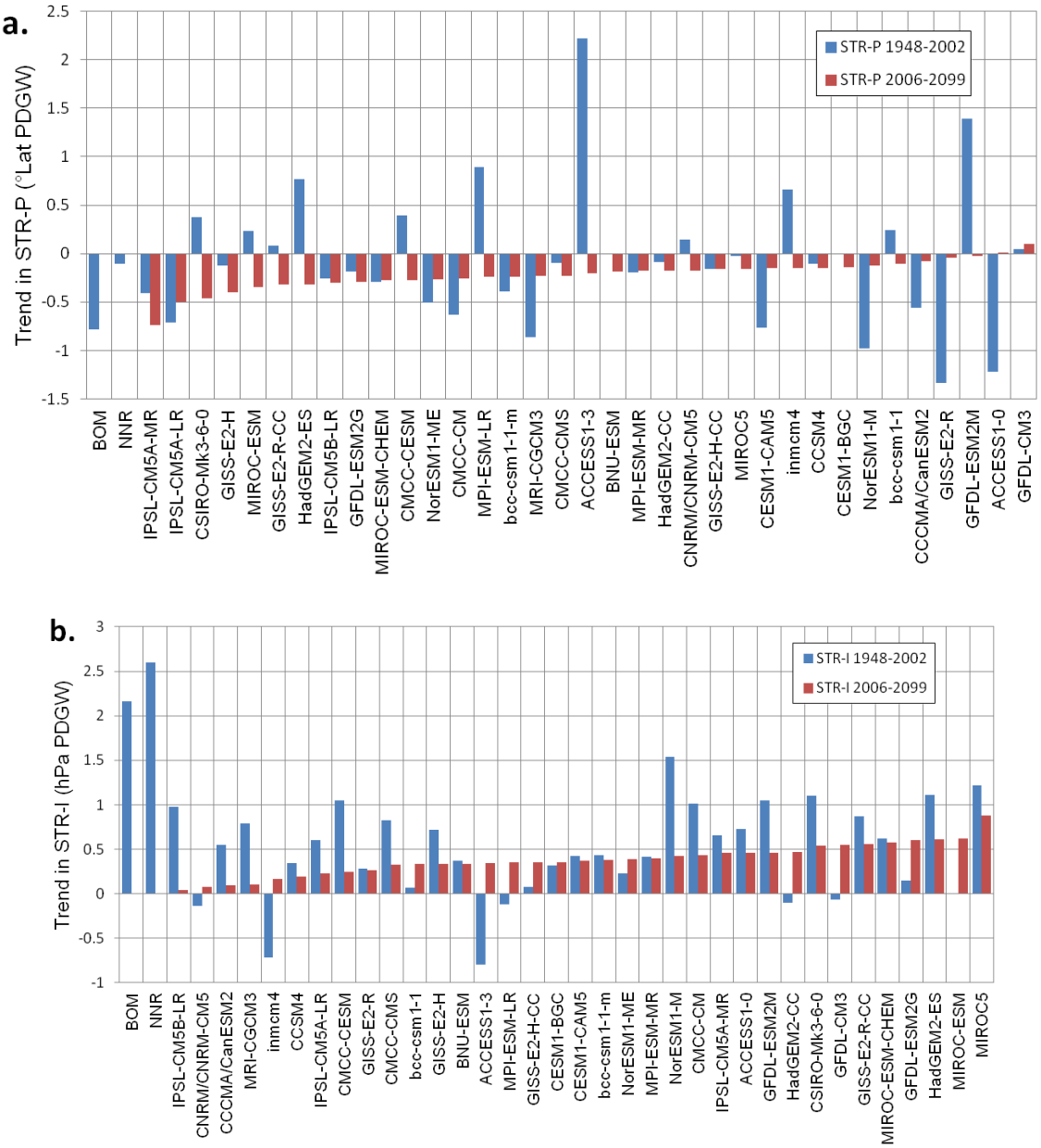

There is no linear relationship between past trends and projected change in STR-I across the range of models (Figure 7a), showing that the strength of past changes is not a good guide to projections. Also, there are no clear distinctions between sub-groups of models, where models that matched NNR in Figure 2 or the group that are candidates for rejection do not show distinct projections from the other models (Table 1). Also, for STR-P there is no statistical relationship between the models' past trend and future trend in or STR-P (Figure 7b), showing that past trends are not a useful constraint on projections of STR-P either. Similar to the relationship between past trends and future trends, there is no significant relationship between the bias in the mean or inter-annual variability compared to BOM or NNR in each model and its projected trend in either STR-I or STR-P (all correlation coefficients of inter-model spread are R<0.1).

Rainfall in the southeast Australia box is projected to decrease in April-October in almost every model (Table 1), which is broadly consistent with a strengthening and pole-ward movement of the STR. However, the relationship between change in STR-I and STR-P and rainfall change is not consistent with observations in each model (as shown in Figure 4 and 5). This difference can also be seen in a scatter plot of rainfall and STR-I (Figure 8). AWAP rainfall totals and STR-I in April-October have a negative correlation in 1950-1999 (50-year periods at the end of each

century are used to illustrate change over the 21st Century). This relationship has a slope of -7.36, where rainfall is 7 mm/month (13% of the observed mean) lower with each hPa of STR strength, and a reasonable fit (correlation coefficient of $R^2 = 0.5$). Models typically do not reproduce this relationship, seen as a smaller slope of the cloud of points (Figure 8). All models show a more intense STR and most models show reduced rainfall by late in the century (2050-2099), shown by the red points (Figure 7). Some models show a negative slope in the past period and future values show generally higher STR-I and lower rainfall in future (e.g. IPSL models), but other models show no slope in the past period and the higher STR-I values in future are associated with a similar magnitude of rainfall (e.g. MIROC models). Similar but weaker relationships are found for STR-P as for STR-I (not shown).

Figure 7 Linear trend in STR indices in each 35 CMIP5 models for the April-October season for 1948-2002 compared to 2006-2099, (a) STR-I and (b) STR-P (fit is shown above each plot); showing models rejected for width criterion (green markers), models rejected for location criterion (blue markers), all other models (red markers), recent trend in BOM (solid red line), recent trend in NNR (dashed red line) and zero line (black). For model key see numbers in Table 1

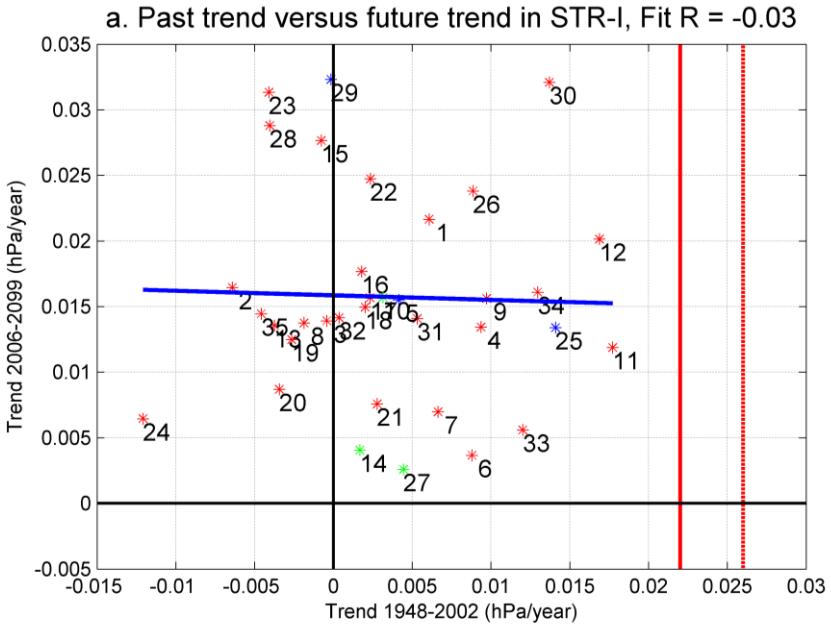

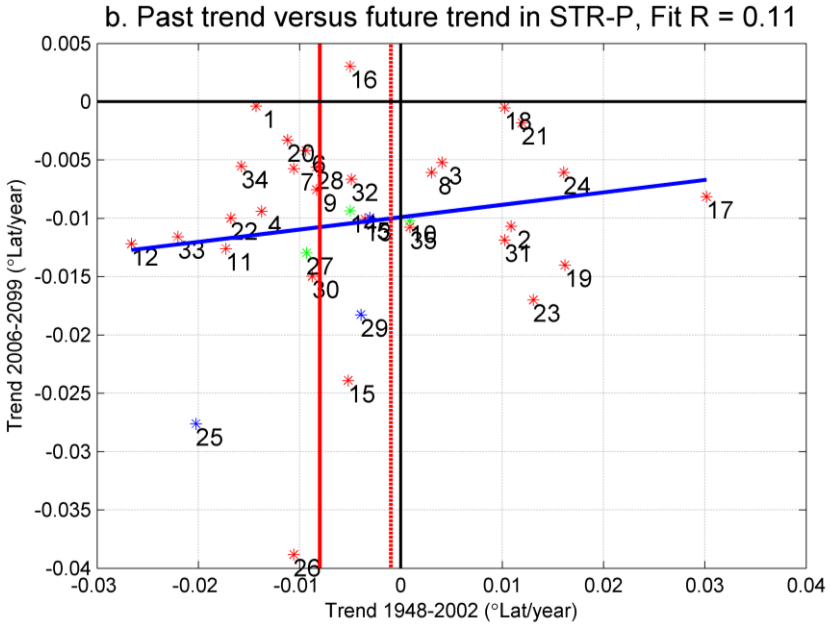

Figure 8 Scatter plot of STR-I index (hPa, x-axis) against rainfall total in the southeast Australian box (mm/month, y-axis) for the April-October season in BOM-AWAP, and 35 CMIP5 models. Blue points are for 1950-1999 and red points are for 2050-2099, linear trend in modelled rainfall over 2006-2099 (mm/month/decade) shown next to model name for reference

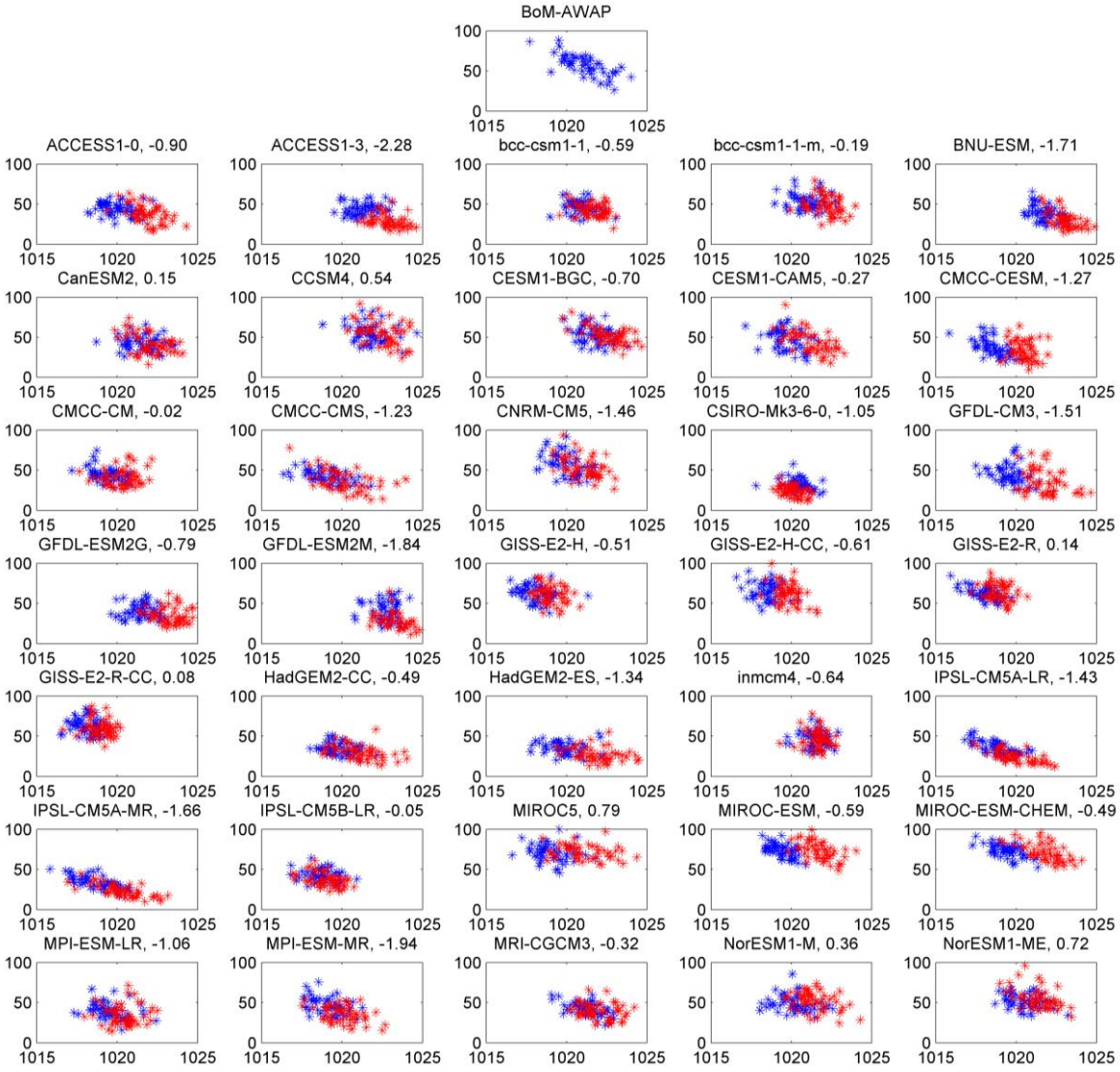

To explore rainfall projections in light of the poor connection between STR-I and rainfall variability, a linear analysis is performed. To infer the rainfall reduction that may be possible from the projected change to STR-I in CMIP5, we can use the observed relationship between STR-I and rainfall. The observed relationship between STR-I and rainfall using inter-annual variability is -7 mm/month per hPa of STR-I (described above), and using trends over 1948-2002 the relationship is similar at -6.45 mm/month per hPa (Table 1). We use the estimate based on trends. The mean projection of STR-I under RCP8.5 is 0.14 hPa/decade (10^{th} to 90^{th} percentile range 0.06 to 0.29 hPa/decade), and this infers a rainfall reduction of -8.5 mm/month (-17.3 to -3.6 mm/month) or -20% (-35 to -8%) over the century. This is a greater mean reduction and smaller model range than that from direct model output of -5.7 mm/month (-15.9 to -2.6 mm/month) or -13% (-40 to +6%). The rainfall reduction inferred from STR-I is on average 6% greater compared to the direct model output, but with a large difference between models (from 24% greater to 18% less). The proportional change is the focus here, as it is in relation to the simulated mean in the current climate so allows for the underestimation of current rainfall in many models.

Discussion

Some incremental improvement in the model mean simulation of the mean annual cycle of the STR between CMIP3 and CMIP5 is seen in these results. For example, the model mean annual cycle of STR-P and STR-I is closer to observations in CMIP5 than in CMIP3. The simulation of

the STR and its connection to rainfall variability is still a source of uncertainty for regional rainfall projections for southern Australia. In particular, recent trends in STR-I are weaker than in observations and many CMIP5 models show a different correlation between the inter-annual variation in STR-I and rainfall anomalies over southern Australia than that seen in observations. Both these issues were also present in many CMIP3 models (Kent et al. 2013). For CMIP5, 6 out of 35 models examined failed to meet the criterion we set of longitude, compared to 5 out of 23 failed in CMIP3.

Figure 9 Change in rainfall (%) for NRM sub-clusters, RCP8.5 1986-2005 to 2080-2099, showing the median (thick line) and 10th to 90th percentile range of model range (bar) for summer (Su), Autumn (Au), winter (Wi) and spring (Sp). Bars show from left to right: (a) 39 models, (b) 33 models not candidates for rejection, (c) 3 models failing STR width, and (d) 3 models failing STR location. Sub-clusters used are: Southern and South Western Flatlands West and east (SSWFW and SSWFE); Rangelands North and South (RN and RS); Murray Basin (MB); Central Slopes (CS); East Coast South and North (ECS and ECN); and Southern Slopes Victoria West, Victoria East, Tasmania West and Tasmania East (SSVW, SSVE, SSTW and SSTE).

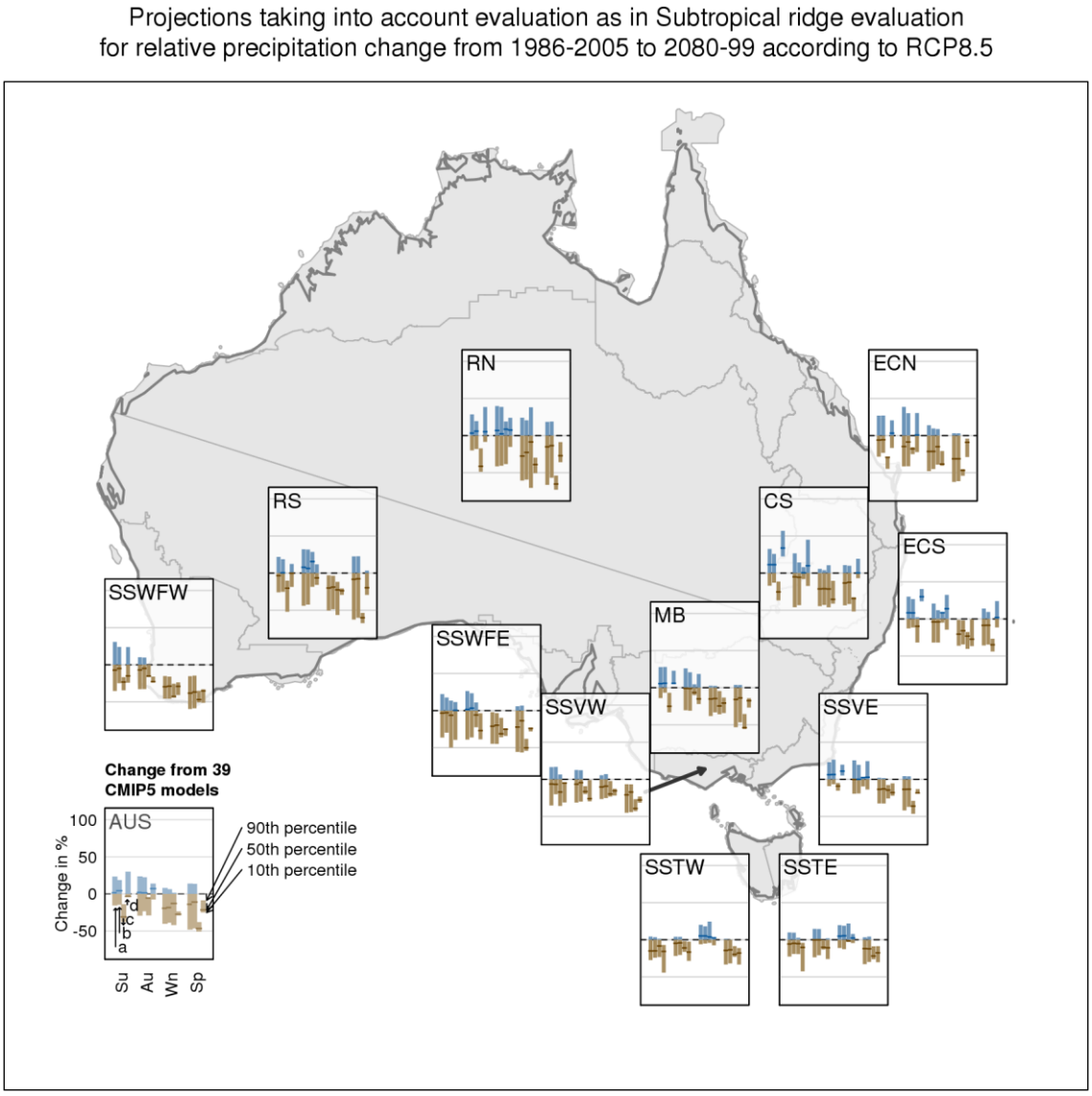

CMIP5 models show an ongoing response of strengthening and pole-ward movement of the STR in the cool season of April-October. This trend is fairly consistent between past and future periods when expressed as trend per degree warming, with the median STR-I trends simulated at around 0.4 hPa and -0.1 °Lat per degree of global warming. There is a spread of trends in the recent past, with some models showing a weaken-

ing and a northerly movement of the STR, but trends are more emphatic in the 21st Century projections. This is likely to be due to the emergence of a strongly forced response from natural variability and noise under this strong forcing scenario.

Across the range of models there are no simple relationships between the projected change in STR-I and simulation of past trends, bias in the mean or bias in the inter-annual variability in the current climate, or the evaluation (the six rejected models did not show a different projection of STR indices to the accepted models). Therefore, there is no clear reason to constrain or weight any part of the modelled range of STR-I projections. Similarly, there are no simple relationships between mean, variability and recent trends in STR-P with its projection, also not supporting a constraint. There is no systematic difference or improvement between Earth System Models (ESMs) and Coupled General Circulation Models (CGCMs). Also, there is no consistently better simulation in models with high spatial resolution.

Trend in STR-I in April-October is underestimated compared to observations in all models. This suggests that the response to forcings is not sensitive enough in models. The influence of natural variability may play a part for any given period and thus explain some of the difference between models and reanalysis as climate models generate their own natural variability which is not timed to the observed variability. However, if the disparity was primarily due to a difference in the phase of natural variability in recent years we would expect to see a match in the trends in at least some models by chance. If the observed trend is itself at the extreme end of the spectrum of natural variability than a very large ensemble of simulation would be required to capture such a trend, but the fact that the trend magnitude is similar over the last 50 years and over the last 110 years suggest that this is unlikely. The consistent underestimation of STR-I trend in all models therefore suggests that is it is a systematic model bias in this response. Also, the CMIP5 models generally simulate the correlation between the STR and southeast Australian rainfall weaker than observations, in some cases with the opposite sign. This raises doubts about the overall magnitude of rainfall change in southeast Australia in response to changes in the STR, and also the spatial pattern of rainfall response. The CMIP5 models simulate a general decline in southeast Australian rainfall in the April-October season under RCP8.5. However, the poor simulation of the STR-rainfall relationship suggests that the rainfall reduction in southeast Australia may also be underestimated in projections. Simple linear analysis infers that the decrease in rainfall from the projected change in STR-I over the century is greater than what the raw model outputs indicate (median projections of -20% compared to -13%). Here we must acknowledge that there are of course other influences on rainfall in southeast Australia other than the influence from STR-I, but this underestimation of rainfall trends appears quite plausible.

The underestimation of recent trends in STR-I also suggests that the projected rainfall changes are underestimated in CMIP5. The observed rate of STR-I change in April-October in the 20th Century is at least 2 hPa per degree warming (2.16, 2.26 and 2.6 hPa PDGW in different datasets, see above), whereas models simulate a fairly consistent trend per degree of warming in the past and future (model median of around 0.4 hPa PDGW in both). This suggests that if the observed trend in STR-I of the 20th Century continues in 21st Century, then this would imply a very marked rainfall decrease. Therefore the projections from GCMs have the potential to underestimate the rainfall change, and that larger changes than the CMIP5 range are possible. Along with a possible under-estimation of the associated rainfall decline, many models are likely to have an incorrect projection of the spatial pattern of rainfall change associated with an intensification or pole-ward movement of the STR in the cool season. The correlation of rainfall to STR indices (Figure 1b and 1c) gives an indication of where the effect could be expected to be the largest. Some models with higher resolution that represent this regional patterns better than other models, such as MRI-CGCM3 (Figure 3), may provide some insights into the regional pattern of rainfall change, and this is worthy of further investigation.

There is no simple clear distinction between the models that fail the longitude test and those that pass in terms of the projection of STR indices or rainfall in southern Australia. However, there is some relationship between evaluation of STR and rainfall projections north of the STR (Figure 8). The width or position of the MSLP patterns that correspond to the observed STR at 140-150 °E in models appears to have a significant effect on rainfall projections, and this also is worthy of further investigation.

References

Cai, W., van Rensch, P. and Cowan, T. 2011. Influence of Global-Scale Variability on the Subtropical Ridge over Southeast Australia. Journal of Climate 24: 6035-6053.

Christensen, J.H. and co-authors 2007. Regional climate projections. Climate Change 2007: The Physical Science Basis. Contribution of Working Group I to the Fourth Assessment Report of the Intergovernmental Panel on Climate Change. S. Solomon, D. Qin, M. Manning et al. Cambridge, United Kingdom, Cambridge University Press.

Collins, M., Arblaster, J.M., Christensen, J.H., Marozke, J., van Oldenborgh, G.J., Power, S.B., Rummukainen, M. and Zhou, T. 2013a. Annex I: Atlas of Global and Regional Climate Projections. Climate Change 2013: The Physical Science Basis. Contribution of Working Group I to the Fifth Assessment Report of the Intergovernmental Panel on Climate Change. T. F. Stocker, D. Qin, G.-K. Plattner et al. Cambridge, United Kingdom and New York, NY, USA, Cambridge University Press.

Collins, M. and co-authors 2013b. Chapter 12: Long-term Climate Change: Projections, Commitments and Irreversibility. Climate Change 2013: The Physical Science Basis. Contribution of Working Group I to the Fifth Assessment Report of the Intergovernmental Panel on Climate Change. T. F. Stocker, D. Qin, G.-K. Plattner et al. Cambridge, United Kingdom and New York, NY, USA, Cambridge University Press.

CSIRO 2012. Climate and water availability in south-eastern Australia – A synthesis of findings from Phase 2 of the South Eastern Australian Climate Initiative (SEACI). CSIRO: 41 pp.

Das, S.C. 1956. Statistical analysis of Australian pressure data. Australian Journal of Physics 9.

Deacon, E.L. 1953. Climatic change in Australia since 1880. Australian Journal of Physics 6: 209-218.

Drosdowsky, W. 2005. The latitude of the subtropical ridge over eastern Australia: The L index revisited. International Journal of Climatology 25: 1291-1299.

Frederiksen, J.S. and Frederiksen, C.S. 2011. Twentieth Century Winter Changes in Southern Hemisphere Synoptic Weather Modes. Advances in Meteorology 2011: 16 pages, doi:10.1155/2011/353829.

Jones, D.A., Wang, W. and Fawcett, R. 2009. High-quality spatial climate data-sets for Australia. Australian Meteorological and Oceanographic Journal 58: 233-248.

Kalnay, E. and co-authors 1996. The NCEP/NCAR 40-year reanalysis project. Bulletin of the American Meteorological Society 77: 437-471.

Karoly, D.J. 2003. Ozone and Climate Change. Science 302: 236-237.

Kent, D.M., Kirono, D.G.C., Timbal, B. and Chiew, F.H.S. 2013. Representation of the Australian sub-tropical ridge in the CMIP3 models. International Journal of Climatology 33: 48-57.

Kidson, E. 1925. Some periods in Australian weather., Commonwealth Bureau of Meteorology (Australia) Bulletin, 17.

Larsen, S.H. and Nicholls, N. 2009. Southern Australian rainfall and the subtropical ridge: Variations, interrelationships, and trends. Geophysical Research Letters 36: 5.

Lucas, C., Timbal, B. and Nguyen, H. 2014. The expanding tropics: a critical assessment of the observational and modeling studies. Wiley Interdisciplinary Reviews: Climate Change 5: 89-112.

Maher, P. and Sherwood, S.C. 2014. Disentangling the Multiple Sources of Large-Scale Variability in Australian Wintertime Precipitation. Journal of Climate 27: 6377-6392.

Meehl, G.A., Covey, C., Delworth, T., Latif, M., McAvaney, B., Mitchell, J.F.B., Stouffer, R.J. and Taylor, K.E. 2007. The WCRP CMIP3 multimodel dataset - A new era in climate change research. Bulletin of the American Meteorological Society 88: 1383-1394.

Nguyen, H., Evans, A., Lucas, C., Smith, I. and Timbal, B. 2013. The Hadley Circulation in Reanalyses: Climatology, Variability, and Change. Journal of Climate 26: 3357-3376.

Peixoto, P. and Oort, H. 1992. Physics of Climate. , Springer.

Pittock, A.B. 1971. Rainfall and the general circulation. Proceedings of the International Conference on Weather Modification. Canberra, Australia, American Meteorological Society: 330-338.

Pittock, A.B. 1973. Global meridional interactions in stratosphere and troposphere. Quarterly Journal of the Royal Meteorological Society 99: 424-437.

Risbey, J.S., McIntosh, P.C. and Pook, M.J. 2013a. Synoptic components of rainfall variability and trends in southeast Australia. International Journal of Climatology 33: 2459-2472.

Risbey, J.S., Pook, M.J. and McIntosh, P.C. 2013b. Spatial trends in synoptic rainfall in southern Australia. Geophysical Research Letters 40: 3781-3785.

Taylor, K.E., Stouffer, R.J. and Meehl, G.A. 2012. An Overview of CMIP5 and the Experiment Design. Bulletin of the American Meteorological Society 93: 485-498.

Thresher, R.E. 2003. Long term trends in the latitude of the sub-tropical ridge over southeast Australia: climate correlates and consequences. Seventh International Conference on Southern Hemisphere Meteorology and Oceanography. Wellington, New Zealand.

Timbal, B. 2009. The continuing decline in South-East Australian rainfall – Update to May 2009. CAWCR Research Letters 2: 4-11.

Timbal, B. and co-authors 2010. Understanding the anthropogenic nature of the observed rainfall decline across South Eastern Australia. Melbourne, Australia, CAWCR Technical report 26, Centre for Australian Weather and Climate Research.

Timbal, B. and Drosdowsky, W. 2013. The relationship between the decline of South Eastern Australia rainfall and the strengthening of the subtropical ridge. International Journal of Climatology 33: 1021-1034.

van Vuuren, D. and co-authors 2011. The representative concentration pathways: an overview. Climatic Change 109: 5-31.

Whan, K., Timbal, B. and Lindesay, J. 2013. Linear and nonlinear statistical analysis of the impact of sub-tropical ridge intensity and position on south-east Australian rainfall. International Journal of Climatology 34: 326-342.

Williams, A.J. and Stone, R.C. 2009. An assessment of relationships between the Australian subtropical ridge, rainfall variability, and high-latitude circulation patterns. International Journal of Climatology 29: 691-709.

Additional Material A Annual cycle of STR-P and STR-I in BOM (blue) and 35 CMIP5 models (red) for 1948-2002 (labels on ACCESS-1.0 show months for all plots: February, April, June, August, October and December).

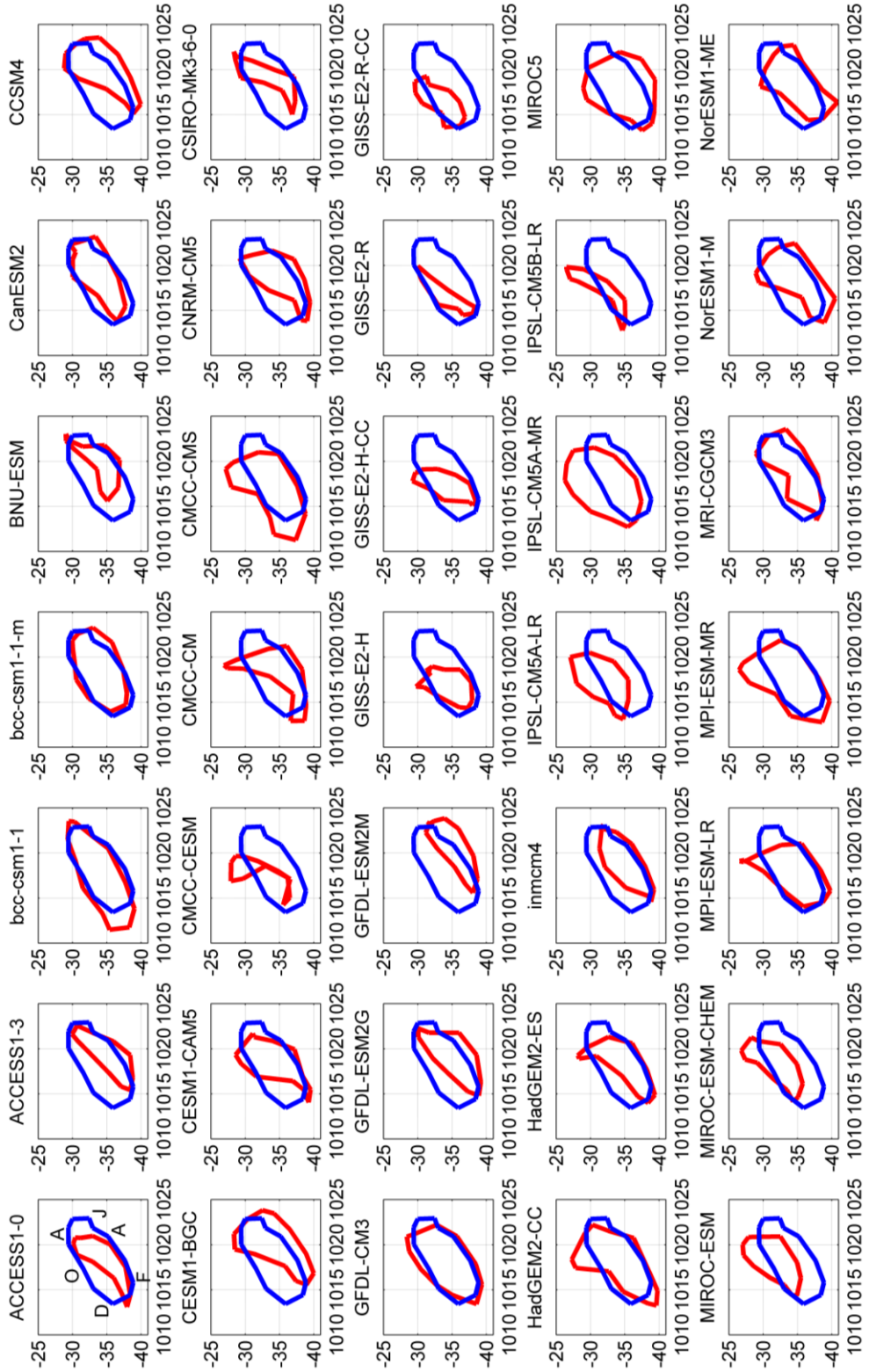

Additional Material B Correlation of AWAP annual rainfall variability and the annual STR-I index in NNR (top left), and the correlation in 35 CMIP5 models